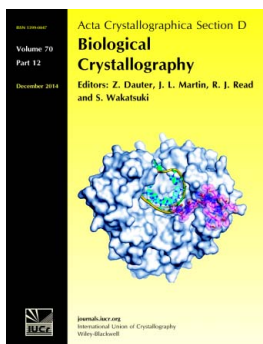# Multi-lamellar organization of fully deuterated lipid extracts of yeast membranes

Yuri Gerelli, Alexis de Ghellinck, Juliette Jouhet, Valérie Laux, Michael Haertlein and Giovanna Fragneto

Acta Crystallographica Section D: Biological Crystallography welcomes the submission of papers covering any aspect of structural biology, with a particular emphasis on the structures of biological macromolecules and the methods used to determine them. Reports on new protein structures are particularly encouraged, as are structure–function papers that could include crystallographic binding studies, or structural analysis of mutants or other modified forms of a known protein structure. The key criterion is that such papers should present new insights into biology, chemistry or structure. Papers on crystallographic methods should be oriented towards biological crystallography, and may include new approaches to any aspect of structure determination or analysis. Papers on the crystallization of biological molecules will be accepted providing that these focus on new methods or other features that are of general importance or applicability.

Crystallography Journals Online is available from **journals.iucr.org**

Multi-lamellar organization of fully deuterated lipid extracts of yeast membranes

Yuri Gerelli,[a]* Alexis de Ghellinck,[a,b] Juliette Jouhet,[c] Valérie Laux,[a] Michael Haertlein[a] and Giovanna Fragneto[a]*

[a]Institut Laue–Langevin, 71 Avenue des Martyrs, 38000 Grenoble, France, [b]Departement de Physique, Faculté des Sciences, Université Libre de Bruxelles, Boulevard du Triomphe CP223, 1050 Bruxelles, Belgium, and [c]Laboratoire de Physiologie Cellulaire et Végétale (LPCV), CNRS (UMR5168)/Université Grenoble Alpes/INRA (USC1359)/CEA Grenoble, Institut de Recherches en Technologies et Sciences pour le Vivant (iRTSV), 17 Rue des Martyrs, 38054 Grenoble CEDEX 9, France

Correspondence e-mail: gerelli@ill.fr, fragneto@ill.fr

Neutron scattering studies on mimetic biomembranes are currently limited by the low availability of deuterated unsaturated lipid species. In the present work, results from the first neutron diffraction experiments on fully deuterated lipid extracts from the yeast *Pichia pastoris* are presented. The structural features of these fully deuterated lipid stacks are compared with those of their hydrogenous analogues and with other similar synthetic systems. The influence of temperature and humidity on the samples has been investigated by means of small momentum-transfer neutron diffraction. All of the lipid extracts investigated self-assemble into multi-lamellar stacks having different structural periodicities; the stacking distances are affected by temperature and humidity without altering the basic underlying arrangement. At high relative humidity the deuterated and hydrogenous samples are similar in their multi-lamellar arrangement, being characterized by two main periodicities of ~75 and ~110 Å reflecting the presence of a large number of polar phospholipid molecules. Larger differences are found at lower relative humidity, where hydrogenous lipids are characterized by a larger single lamellar structure than that observed in the deuterated samples. In both cases the heterogeneity in composition is reflected in a wide structural complexity. The different behaviour upon dehydration can be related to compositional differences in the molecular composition of the two samples, which is attributed to metabolic effects related to the use of perdeuterated growth media.

1. Introduction

Membranes surrounding cells or present inside cells consist of a complex mixture of lipids and proteins. Lipids are amphiphilic molecules that form a continuous bilayer, which acts as a barrier to water-soluble molecules and provides the skeleton for the incorporation of membrane proteins, and they can represent a large fraction of the membrane components (Spector & Yorek, 1985). Their spatial organization within a membrane is strongly related to functionality. For example, it is known that in nature the phospholipid distribution across the inner and outer leaflets of cell membranes is asymmetric (Devaux, 1991, 1992; Van Meer *et al.*, 2008) and that this asymmetry is important for certain cellular processes. As an example, the interaction between phosphatidylserine lipid molecules located in the inner leaflet and skeletal proteins such as spectrin improves the mechanical stability of the membranes of red blood cells (Manno *et al.*, 2002; Ikeda *et al.*, 2006). Clearly, the overall membrane functionality is not provided by lipid molecules alone but occurs as a result of complex interplay between all constituents (proteins, enzymes *etc.*). Because of the complexity of cell membranes, their

3167

structural characterization on the nanometre scale is challenging. Consequently, membrane biophysics has moved its focus over the years from the study of mono-component synthetic lipid bilayers to that of complex systems that more closely mimic the composition of natural membranes. Scattering techniques have been widely employed for the investigation of the subnanometre features of such systems.

In the last thirty years, a wide variety of systems optimized for different structural techniques have been developed (Simons & Vaz, 2004; Safinya *et al.*, 1986). These have provided important information on lipid–lipid, lipid–peptide and lipid–protein organization and interactions. Considerable effort is now being focused on the exploration of increasingly complex systems such as bilayers containing phospholipids with various degrees of unsaturation, sterols and gangliosides. These are interesting because it has been suggested that a number of cellular processes are mediated by lipid domains (or rafts) (Simons & Ikonen, 1997). These domains may have a different lipid composition in comparison with that of the surrounding membrane, and also host proteins or receptors suited for such a lipid environment. In this context, neutron and X-ray scattering techniques can provide information on structure and dynamics on length scales and timescales relevant to the study of model cell membranes. In particular, cold neutrons having wavelengths in the range from 3 to 20 Å are ideal tools for the structural characterization of lipid bilayers, and unlike X-rays they are nondestructive and sensitive to light elements. Furthermore, since neutrons interact weakly with atomic nuclei, they can penetrate many materials, allowing the use of complex sample environments as well as *in situ* measurements on buried interfaces.

Neutron diffraction measurements can be used to study periodic systems, yielding information on the scattering length density (SLD) profile of the sample along a definite direction. Small momentum-transfer diffraction is also widely used to study molecular stacks with well defined periodicities. For the study of model membranes, multi-lamellar systems consisting of several hundred bilayers are required for measurable diffraction from samples with good planar orientation (typically less than a few degrees). Small momentum-transfer neutron diffraction is also a powerful technique for the study of the location of guest molecules within the lipid bilayer, for example cholesterol or peptide molecules (Zaccai *et al.*, 1979; Büldt & Seelig, 1980), as well as for the study of hydration and temperature effects on the structure of membranes. In the case of biological samples, which are inherently rich in hydrogen, dramatic changes in scattering amplitudes are achieved through the substitution of hydrogen by its isotope deuterium. This allows contrast-variation methods (Jacrot, 1976) to either highlight or match the scattering from particular regions of a system, something that can be particularly useful in the case of complex systems.

Despite the power of these neutron techniques, the use of biological cell membranes is limited by the availability of sufficient quantities of deuterated lipids. The use of deuterated lipids has great potential for structural studies of membrane proteins in their natural lipid environment (Maric, Skar-

Gislinge *et al.*, 2014; Maric, Thygesen *et al.*, 2014). A very limited amount of structural data has been published on native cell membranes or native-like synthetic mixtures. To our knowledge, there are only a few examples in the literature of neutron diffraction studies of the role of hydration in natural lipids (McDaniel, 1988; Sebastiani *et al.*, 2012; Demé *et al.*, 2014), although membrane-characterization work on bacteriorhodopsin on purple membranes (PMs; Blaurock & Stoeckenius, 1971; Henderson, 1975, 1977; Dencher *et al.*, 1989) has mainly focused on the characterization of the membrane protein itself. Other examples of the application of diffraction techniques to the study of natural membrane systems include myelin (Kirschner & Caspar, 1972) and egg lecithin (Zaccai *et al.*, 1975; Cowley *et al.*, 1978) membranes. In particular, the work of Cowley and coworkers focused on the study of the repulsive forces between adjacent egg lecithin bilayers in the presence of a large quantity of anionic phospholipid molecules and in the absence of added salts (zero ionic strength). Grage *et al.* (2011) have also used small-angle neutron scattering (SANS) and reflection approaches, in conjunction with protein denaturation and a wide range of other techniques, to study a membrane-embedded mechanosensitive channel protein system.

In contrast to the small number of studies of natural systems, bilayers from synthetic lipids have been widely investigated to study phase behaviour, water permeability and the changes induced by membrane proteins (Stoker *et al.*, 1978; Gordeliy & Chernov, 1997; Nagle & Tristram-Nagle, 2000; Gawrisch *et al.*, 2007). The use of synthetic lipids was necessary to obtain well defined and homogeneous lamellar structures, thus increasing the level of detail in structural characterization. The hydration of bilayers is interesting because the stability of the system results from the hydrophobic effect, which promotes an increase in the free energy of water upon contact with hydrophobic hydrocarbon chains (Tanford, 1980) and a substantial repulsive pressure between bilayers (LeNeveu *et al.*, 1976). Moreover, fluid lipid bilayers, and in particular those having polyunsaturated chains (Huster *et al.*, 1997), have a surprisingly large permeability for water molecules. This is an important aspect because natural lipids are mostly composed of unsaturated and polyunsaturated molecules (Spector & Yorek, 1985). Among the phospholipids, 1-palmitoyl-2-oleoyl-*sn*-glycero-3-phosphocholine (POPC) is of particular interest because the oleic fatty acid (C18:1) is one of the major lipid components in cell membranes (Spector & Yorek, 1985).

The effect of hydration water on pure POPC stacked membranes has been investigated by neutron diffraction and nuclear magnetic resonance (Gawrisch *et al.*, 2007), showing that water could penetrate into the bilayers down to the level of hydrocarbon-chain carbonyl groups, while water content in the hydrophobic bilayer centre was not detectable. This sort of system does not provide a good model for natural membranes given that it does not contain the negative charges in the hydrophilic headgroup region. A more relevant system was described by Cowley *et al.* (1978). These authors found that the presence of a large amount of anionic phospholipids, such

as phosphatidylglycerol (PG), to zwitterionic phospholipids, such as phosphatidylcholine (PC), induces swelling of the bilayer stack. In the case of zero ionic strength, electrostatic repulsion between neighbouring bilayers has been shown to be the main repulsive force, promoting very large bilayer-to-bilayer separations (Cowley *et al.*, 1978; Schneck *et al.*, 2011; Steiner *et al.*, 2012).

As described below, the natural lipid extracts investigated in the current experiments were a mixture of different lipid moieties that could be described as a zwitterionic matrix containing ∼25% anionic lipid molecules. All of the measurements were carried out in ultrapure H_2O/D_2O mixtures, *i.e.* under similar conditions to those used by Cowley and coworkers. The present work involves the use of natural deuterated lipids extracted from organisms grown in deuterated media. This allows the production of grams of natural deuterated material, making full use of the Deuteration Laboratory platform at the ILL. The structural characterization of these lipid extracts and their comparison with model synthetic systems will be valuable and important to find the relationship between the plethora of existing structural studies of model membrane systems and the function of real cell membranes.

In this paper, the first structural characterization of fully deuterated lipid extracts from *Pichia pastoris* yeast cell membranes is presented together with a study of the effect of temperature and hydration on these systems. For comparison purposes, hydrogenous extracts obtained under the same conditions have also been analyzed. Compositional analyses of both types of extract have recently been described by de Ghellinck *et al.* (2014). It must be noted that one step of this analysis involved a methylation process (Ichihara & Fuku-bayashi, 2010; de Ghellinck *et al.*, 2014). During this step the phospholipid molecules were broken into hydrophilic (head-group) and hydrophobic (fatty acids) fragments. Commonly two (or three in the case of cardiolipin) fatty-acid chains are attached to a single headgroup. Since for a given headgroup type the combination of fatty-acid chains can vary, and since the individual fatty-acid species were extracted after detaching them from the headgroup, the determination of the constitu-ents as an entire molecule in terms of headgroup and chain pairs and triplets remained unknown. It is nevertheless clear that there were differences in fatty-acid composition between hydrogenous and deuterated extracts (de Ghellinck, 2013; de Ghellinck *et al.*, 2014). These differences have been attributed to metabolic effects related to the use of perdeuterated growth media, and give rise to different bilayer structures for the hydrogenous and deuterated extracts (de Ghellinck *et al.*, 2014) and to a different organization of the multi-lamellar stacks, as described in the present work.

In order to use these extracts in more advanced scattering studies (interaction with other molecules such as peptides or drugs, for example) a full characterization of their organiza-tion under different experimental conditions and a compar-ison of the effects of the compositional differences between hydrogenous and deuterated analogues is essential. Despite the intrinsic disorder of a fluid complex lipid mixture that leads to 'poor' diffraction data (Rappolt, 2010), important conclusions may be drawn from a comparison of these data with those from standard model systems.

2. Materials and methods

2.1. Yeast culture

Perdeuterated lipids were extracted from the methylo-trophic yeast *P. pastoris* grown at 30°C in flask cultures. Fully deuterated minimal medium based on basal salt medium (BSM) pH 6.0 (*Pichia* fermentation process guidelines, Invitrogen, USA) containing 20 g l⁻¹ glycerol-d$_8$ (Euriso-Top, France) was used as a carbon source. *P. pastoris* cells were harvested by centrifugation at the end of the logarithmic phase at an optical density OD_{600} of about 80. Hydrogenated extracts were produced according to the same protocol but using hydrogenous glycerol and H_2O in the growth media. Further details can be found in the literature (de Ghellinck *et al.*, 2014).

2.2. Lipid extraction

Deuterated yeast cells were produced in the Deuteration Laboratory (D-Lab) within ILL's Life Science Group. They were harvested at the end of the logarithmic phase and poured into boiled ethanol in order to block the action of endogenic enzymes able to damage glycerophospholipids. Lipids were then extracted according to the method of Folch *et al.* (1957). The phospholipid composition was established by two-dimensional thin-layer chromatography and was quantified by GC-FID as described in Jouhet *et al.* (2003).

2.3. Sample preparation

Thin silicon wafers (40 × 30 × 0.5 mm) were cleaned by soaking in acetone, ethanol and HPLC-grade chloroform (Sigma–Aldrich, USA), each time under sonication. Dry lipids (30 mg) were dissolved in 20 ml chloroform and the entire solution was then deposited onto the wafers using the 'rock and roll' method (Tristram-Nagle, 2007). It is known that rapid evaporation of the solvent might create surface defects and poor orientation of the stacked membranes. To avoid these effects, the entire preparation process was performed in a cold room (8°C). Orientation of the bilayers parallel to the cover-slip was enhanced by drying them for 24 h under vacuum at 40°C. Subsequently, they were rehydrated in a fully saturated D_2O atmosphere, without addition of salts, for 48 h.

2.4. Neutron diffraction

A typical diffraction pattern is characterized by a series of diffraction peaks according to Bragg's law and provides the following information: (i) the number of diffraction peaks gives an indication of the ordering of the sample, which can come from the choice of the system or from the quality of the sample preparation, (ii) the angular position of the peaks relates to the periodicity of structural features in the corresponding direction and (iii) for each observation the

Table 1
Temperatures of the sample, T_s, and water reservoir, T_r, and the resulting hydration levels used in the experiment. LRH and HRH stand for low relative humidity and high relative humidity, respectively.

	T_s (°C)	T_r (°C)	RH (%)
HRH	18	16	82
	30	28	87
	60	58	90
LRH	18	8	20
	30	20	40
	60	50	59

integrated intensity of the peak is proportional to the square of the structure-factor modulus once corrections have been applied (*e.g* absorption, Lorentz and geometrical corrections). The SLD profile in real space (in the plane of incidence of, *i.e.* normal to, the sample surface) can be derived from a Fourier synthesis based on the structure factors. The absolute resolution is generally low and depends on the extent of the diffraction peaks in reciprocal space.

Neutron diffraction experiments were performed on the small momentum-transfer diffractometer D16 at the Institut Laue–Langevin (ILL), Grenoble, France. The wavelength and the sample-to-detector distance were 4.752 Å and 0.950 m, respectively. Mono-crystalline silicon wafers (4×3 cm) were mounted vertically on a goniometer head and were illuminated by a neutron beam of dimensions 20×4 mm (height $\times$ width). The angular position of the diffraction peaks was searched by coupled θ–2θ scans, where both the sample and detector angles (θ and 2θ, respectively) were changed. Once the peaks had been found, rocking curves were collected for a fixed 2θ scattering angle while changing the sample angle. Typical rocking curves acquired on the two-dimensional position-sensitive detector are shown in Fig. 1. The two-dimensional rocking curves were integrated along the y axis and converted into $I(Q)$, where $Q = (4\pi/\lambda)\sin(\theta)$ is the wavevector transfer, λ is the wavelength and 2θ is the scattering angle. The conversion between the peak position (reciprocal space) and distances (real space) is $d = 2\pi/Q$.
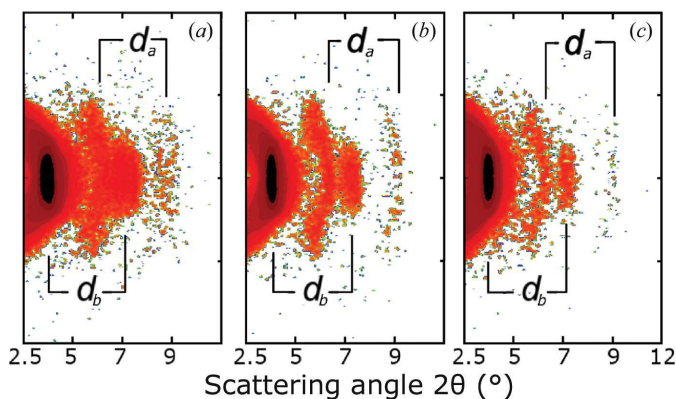
Figure 1
Collection of rocking curves (θ scans) resulting in two-dimensional detector images for H_2O-hydrated samples measured at low RH and at three different temperatures: 18°C (*a*), 30°C (*b*) and 60°C (*c*). Shifts and intensity changes of the main peaks are visible. Their assignment is discussed in detail in the text.

A humidity chamber, consisting of two thermally insulated compartments that could be kept at different temperatures by water circulation, allowed the simultaneous control of relative humidity (RH) and temperature (Perino-Gallice *et al.*, 2002). This was possible by changing the temperature of the water reservoir and of the upper part of the cell. D_2O, H_2O and a 1:1(*v:v*) D_2O:H_2O mixture (called HDO in the following) were used as hydration media. Both temperature and hydration effects were studied. The humidity level was monitored using a commercial humidity sensor (IH-3610-1; Honeywell Inc., USA) placed inside the cell. After temperature stabilization the equilibration of the sample to new humidity levels was followed for 2 h before starting the acquisition of the diffraction pattern. The thermodynamic conditions used are summarized in Table 1.

Angular scans were performed to collect the diffraction patterns of the empty cell, silicon wafer and samples. In this way Bragg peaks arising from the holder and substrate were properly removed from the sample data sets. Background corrections were performed at a later stage.

3. Data analysis

The first result in a diffraction experiment on membrane stacks is the lamellar d-spacing, *i.e.* the repetition distance between two equivalent points of the stack. For a simple stack of bilayers $d = t_B + d_w$, where t_B is the bilayer thickness and d_w is the gap, usually filled with water molecules, between two subsequent bilayers in the stack. Theories describing the diffraction from a stack of membranes have been described for paracrystalline (Guinier, 1963), Caillé-modified (Caillé, 1972; Zhang *et al.*, 1994) or Nallet (Nallet *et al.*, 1993) situations. These approaches were needed because in stacks of pure lipid membranes it is usually difficult to observe high-number diffraction orders, since thermal fluctuations tend to degrade long-range ordering. Moreover, for systems composed of a mixture of lipid molecules, the number of orders of diffraction tends to decrease as a result of compositional heterogeneity. The present paper deals with natural lipid extracts, where the presence of lipids with different sizes, charges and properties reduces this order even more and results in a limited number of visible peaks. In neutron diffraction studies of natural membranes, less than three or four orders of diffraction are typically visible. The only possible analysis is the determination of the lamellar spacing, d, obtained by fitting the peak positions of the hth diffraction order according to Bragg's law

$$d = \frac{h\lambda}{2\sin(\theta)}. \tag{1}$$

The diffraction data were analyzed using the *PeakFit* software (Systat Software) in terms of a sum of Gaussian line shapes, each ascribed to a single peak. The generic fitting function was therefore

$$I(Q) - I_{bkg} = \sum_{h=1}^{h_{max}} a_h \exp\left[-\frac{1}{2}\left(\frac{Q - Q_h}{\sigma_h}\right)^2\right], \tag{2}$$
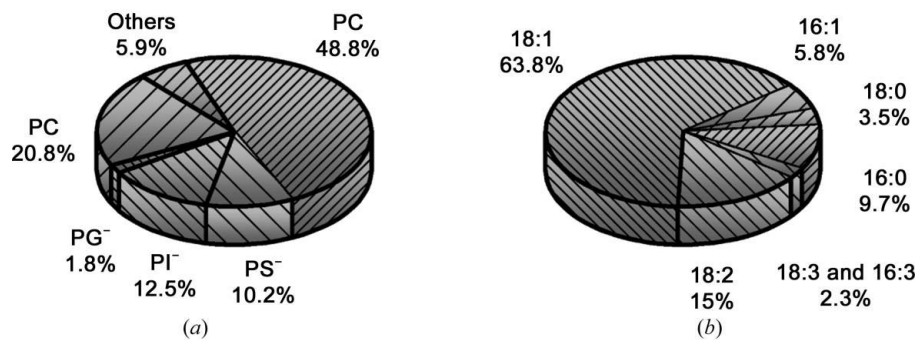
Figure 2
Headgroup and chain distributions for deuterated yeast membranes as determined by chromatography. The acronyms are described in the text. In (b) some elements are grouped to improve visibility.

where a_h, Q_h and σ_h are the amplitude, the position and the width [FWHM$_h$ = 2(2ln2)$^{1/2}\sigma_h$] of the hth peak, respectively. I_{bkg} is a pseudo-exponential background described in terms of diffuse scattering; its shape was determined from the empty holder measurements, and for a proper subtraction only a scaling of the intensity was necessary. Another piece of information that can in principle be derived from the diffraction pattern is the SLD profile of the bilayer in the plane of incidence (Zaccai *et al.*, 1975; Worthington, 1969; King & White, 1986). Because of the intrinsic limitations imposed by the nature of the samples, it was possible to attempt a derivation of the bilayer profile for one sample only, where the third order of diffraction was present. This part of the analysis is explained in detail in §4.3.

4. Structural characterization

Despite the extensive use of *P. pastoris* in biotechnology, fundamental structural investigations of its lipid components are rare (Faber *et al.*, 1995). It was recently shown that the growth mechanism of *P. pastoris* cells is affected by the use of deuterated media instead of hydrogenous media (de Ghellinck *et al.*, 2014). It was hypothesized that the action of fatty-acid desaturase was partially inhibited if deuterated media are used. In hydrogenous extracts oleic (C18:1), linoleic (C18:2) and γ-linoleic (C18:3) fatty acids were found in similar amounts. In deuterated extracts oleic fatty acid was the main hydrophobic component, comprising more than 60% of the total fatty-acid composition. The headgroup and chain distributions obtained from the chromatographic analysis are summarized in Fig. 2 for the deuterated extracts, which constitute the main object of the present work. The detailed composition of the analogous hydrogenous extracts is given elsewhere (de Ghellinck *et al.*, 2014).

The main components were characterized, in terms of polar region, by zwitterionic molecules, namely phosphatidylcholine (PC; ∼50%) and phosphatidylethanolamine (PE; ∼20%), and by negatively charged molecules such as phosphatidylserine (PS; ∼10%) and phosphatidylinositol (PI; ∼10%). For all headgroup moieties the most common chain type was that of

oleic acid (C18:1), representing ∼64% of the total chain distribution. For the polar lipid molecules the most abundant fatty-acid species was myristic acid (C16:0), representing ∼20% of the fatty-acid distribution for PS and PI molecules. As in the case of hydrogenous extracts, the presence of a low amount of sterols and sphingolipids was also detected (Wriessnegger *et al.*, 2009) but was not analysed in detail (de Ghellinck *et al.*, 2014). It is noted that this compositional analysis method, based on methylation of the fatty acids (Ichihara & Fukubayashi, 2010; de Ghellinck *et al.*, 2014), has the drawback that it is impossible to determine the components as entire molecules in terms of headgroup and chains. Only a statistical approach based on the free fatty-acid distributions is possible. This aspect imposes several limitations on the interpretation of neutron diffraction patterns, as the real molecular composition of the samples was unknown.

4.1. Deuterated extracts at high relative humidity

Temperature-induced changes in the multi-lamellar arrangement of the bilayers were investigated by keeping the humidity levels constant in the range 82–90%. In Fig. 3 the diffraction patterns for deuterated membranes measured at three temperatures in H$_2$O are compared. At 18°C two sets of peaks were found; these were attributed to two different lamellar spacings called *a* and *b* (blue and red peaks, respectively, in Fig. 3). First-order diffraction peaks were found at Q_a = 0.061 (1) Å^{-1} and Q_b = 0.082 (3) Å^{-1}, with corresponding periodicities ΔQ_a = 0.060 (1) Å^{-1} and ΔQ_b = 0.083 (3) Å^{-1}, respectively. For the *a* structure three orders of diffraction were observed in H$_2$O, while only two were present for the HDO-hydrated and D$_2$O-hydrated samples. This is not surprising since the scattering contrast is higher between deuterated lipids and H$_2$O than it is between deuterated lipids and D$_2$O. For the *b* pattern two orders of diffraction were observed in H$_2$O and in HDO, while in D$_2$O only the first order of diffraction was visible. By increasing the temperature to 30°C the number of detectable peaks decreased but the position of the visible peaks was unchanged, indicating the presence of the same structural periodicity as observed at the lower temperature. At 60°C the scattering intensity was strongly reduced for all of the contrasts and the *b* pattern disappeared completely, while the *a* pattern was still visible.

Typical fits obtained by using (2) to derive the peak positions are shown in the upper part of Fig. 3. The two main characteristic distances (*d*-spacings) of the sample were derived as d_a = 105 (2) Å and d_b = 76 (3) Å.

4.2. Deuterated extracts at low relative humidity

The diffraction patterns of the deuterated samples changed as the relative humidity level was lowered. As shown in Table

1, the humidity level of the sample was not constant at different temperatures and these differences were reflected in the experimental data, especially at low temperature. In Fig. 1 the rocking-curve temperature evolution of a deuterated sample measured at low RH is displayed. At 30 and 60°C the diffraction patterns are only marginally affected by the small
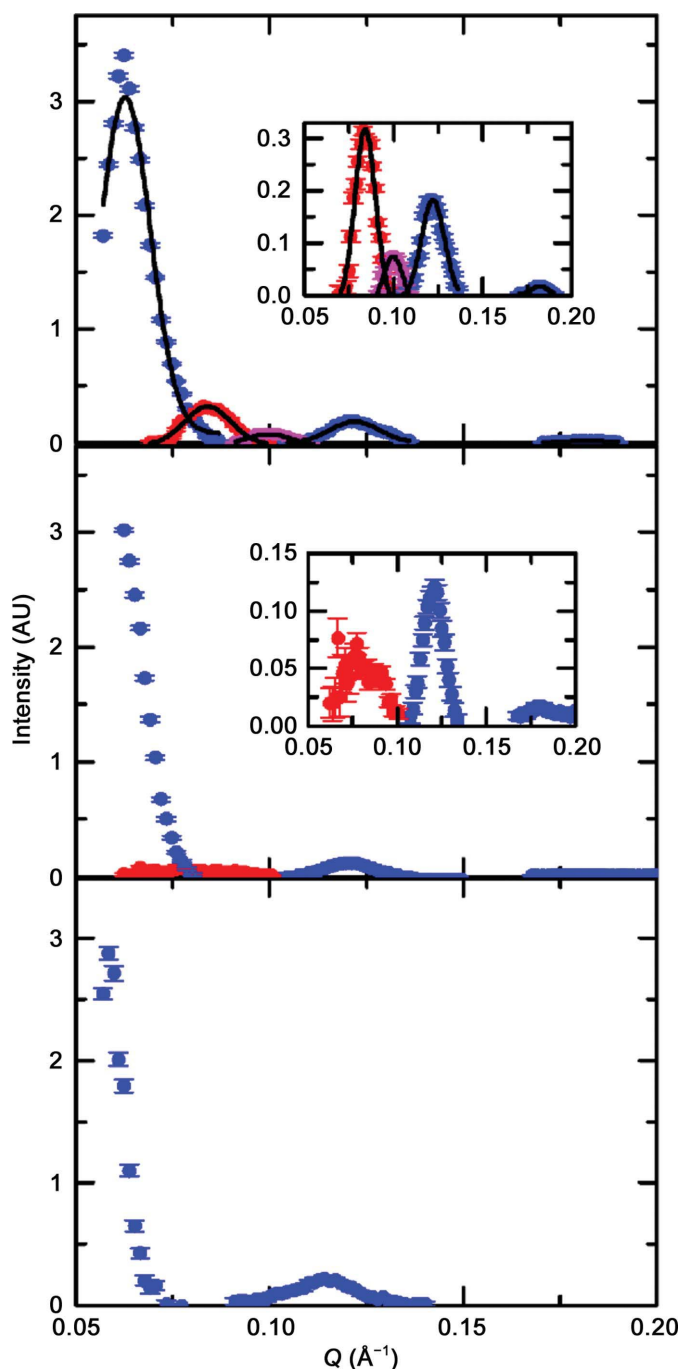
Table 2
Main d-spacing values for deuterated and hydrogenous lipid extracts.

The hydrogenous samples measured at high relative humidity were characterized by two additional d-spacings of 60 ± 1 and 95 ± 2 Å. They were excluded from the table for simplicity.

Temperature (°C)	Deuterated				Hydrogenous		
	HRH		LRH		HRH		LRH
	d_a (Å)	d_b (Å)	d_a (Å)	d_b (Å)	d_a (Å)	d_b (Å)	d_a (Å)
18	105 ± 2	76 ± 3	90 ± 10	72 ± 5	109 ± 1	71 ± 1	103 ± 1
30	105 ± 2	76 ± 3	86 ± 5	73 ± 2	–	71 ± 1	103 ± 1
60	104 ± 2	–	82 ± 6	74 ± 2	109 ± 1	–	103 ± 1

changes in relative humidity. In the low RH case the overall diffracted intensity was lower than that observed in the high RH case. Nevertheless, two diffraction patterns are clearly visible. The predominant set of peaks is characterized by a separation $\Delta Q_b = 0.084\,(2)$ Å^{-1}. The additional pattern, characterized by two secondary peaks centred at $Q_a' = 0.147\,(3)$ Å^{-1} and $Q_a'' = 0.224\,(3)$ Å^{-1}, is present for all samples. In this case the separation is $\Delta Q_a = 0.077\,(6)$ Å^{-1}. A first-order diffraction peak would have been expected at $Q_a = 0.077\,(6)$ Å^{-1}, but it was not observed in any of the samples, probably because it was masked by the very intense first-order peak ascribed to the d_b structure. According to this interpretation the resulting d-spacings were $d_a = 82\,(6)$ Å and $d_b = 75\,(2)$ Å, as reported in Table 2. It must be noted that for the low-temperature measurements (18°C) the diffraction pattern was not clearly defined. In fact the very low level of hydration decreased the regularity of the periodicity, giving rise to wider and less defined peaks (see Fig. 1a). This effect may occur as a result of a reduced water content between subsequent bilayers.

4.3. Hydrogenated extracts at high relative humidity

Stacks of hydrogenous lipid extracts were measured, as a reference, under the same thermodynamic conditions as for the deuterated extracts. In Fig. 4 a collection of diffraction data measured at 18 and 60°C (Figs. 4a and 4b, respectively) and at high relative humidity for hydrogenous and deuterated analogues are compared. At the lower temperature (18°C) the diffraction pattern of hydrogenous lipids contained similar features to those observed for the deuterated extracts under the same thermodynamic conditions (see Fig. 4a). The main difference is a shift in the Q-position of some peaks (blue and red peaks in Fig. 4a), indicating a $\sim$5% change in the d_a and d_b distances (see Table 2). Another difference between the two samples is the absence of the low-Q peak observed for deuterated extracts and an increase in the intensity of the peak at $Q \simeq 0.105$ Å^{-1} (labelled in pink), which was almost invisible in the deuterated extracts measured at high RH at 18°C. It is interesting to note that this was, in terms of intensity, the predominant feature of the diffraction patterns for all of the hydrogenous extracts measured at high relative humidity (see Fig. 5). This is an indication that the peak must originate from a lamellar arrangement that is temperature independent over

Figure 3
Diffraction data for the deuterated samples hydrated in H$_2$O at high relative humidity and at 18, 30 and 60°C (top to bottom). For the data obtained at the lowest temperature the fits obtained using (2) are shown as continuous lines. The peaks belonging to the same set are plotted using the same colour across the three panels: blue for the d_a periodicity and red for the d_b periodicity. At 18°C an unassigned peak was detected (pink dots). Its presence is further discussed in §4.3.

the range covered in this work. The periodicity associated with this feature is $d \simeq 60\,(1)$ Å. Such a value is compatible with the typical d-spacing values found for stacks of zwitterionic natural (Zaccai *et al.*, 1975; Cowley *et al.*, 1978) and synthetic (Cavalcanti *et al.*, 2007; Trapp *et al.*, 2010; Schneck *et al.*, 2011; Steiner *et al.*, 2012; Foglia *et al.*, 2012; Knoll *et al.*, 2014) phospholipid bilayers. At higher temperatures (the middle and bottom panels in Fig. 5) peak-intensity changes were detected. Some peaks became more intense while others were reduced in intensity, but in both cases their positions were almost unaffected by temperature changes. Additional features were nonetheless observed in the data collected at 30 and 60°C, suggesting the presence of a further d-spacing of about 95 Å ($Q \simeq 0.066$ Å^{-1}).

4.4. Hydrogenated extracts at low relative humidity

For the hydrogenous samples measured at low relative humidity (data not shown), the diffraction patterns were much simpler because of the presence of only one well defined
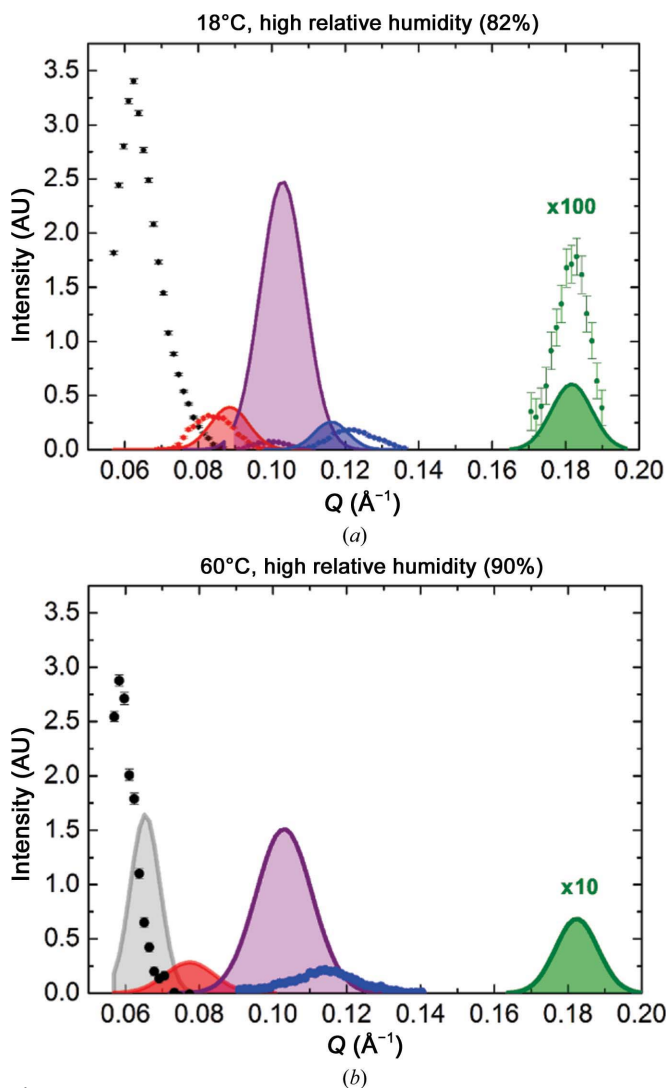

Figure 4
Comparison of high relative humidity diffraction data collected at (*a*) 18°C and (*b*) 60°C for deuterated (symbols) and hydrogenous (shaded areas) lipid extracts.

temperature-independent set of peaks. The Q separation was $\Delta Q = 0.061(1)$ Å^{-1}, corresponding to a real-space distance $d = 103\,(1)$ Å.

4.5. Internal structure of the lipid bilayer

Information on the local structure of lipid bilayers in a multi-lamellar stack was extracted from the neutron diffraction data by exploiting contrast variation, *i.e.* by acquiring the diffraction pattern in at least three media characterized by different H/D isotopic contents (Zaccai *et al.*, 1975; Worthington, 1969; King & White, 1986). In general, the scattering length density profile of a periodic unit with a stacking distance d can be determined from a Fourier synthesis using the observed structure-factor amplitudes $F(h)$ as coefficients (Rappolt, 2010; King & White, 1986),

$$\rho(z) \propto F(0) + \frac{2}{d}\sum_{h=1}^{N} F(h)\cos\left(\frac{2\pi h z}{d}\right), \qquad (3)$$

where N is the maximum order of diffraction detected. The signs of the coefficients $F(h)$ were determined from the intensity changes of the hth-order diffraction peak upon
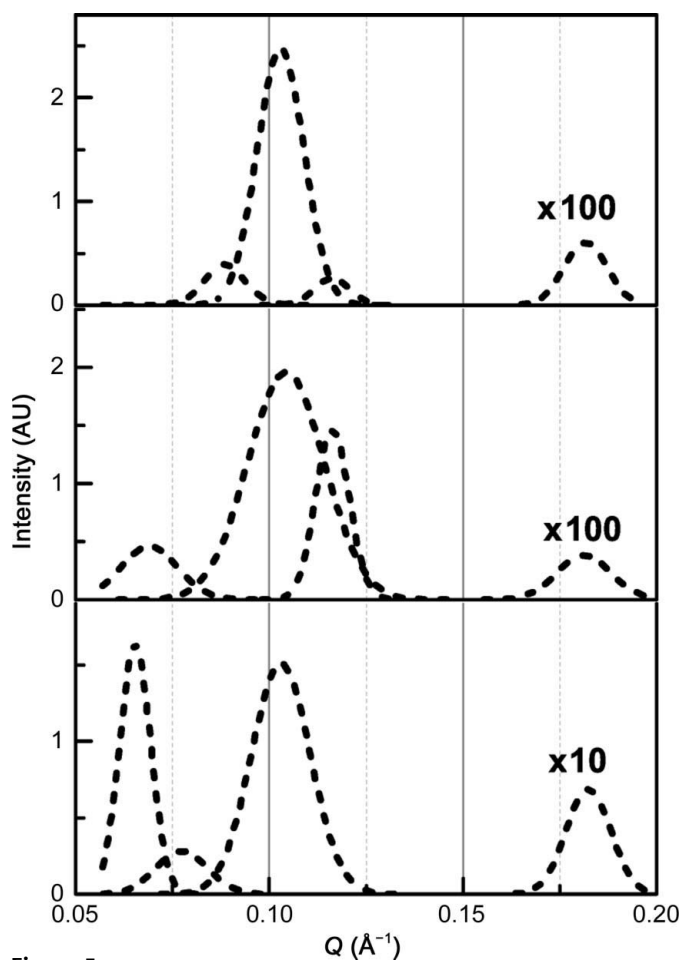

Figure 5
Background-subtracted diffraction data for hydrogenous extracts (high RH HDO) measured at 18, 30 and 60°C (from top to bottom). One of the more intense diffraction peaks measured for these hydrogenous extracts, located at $Q \simeq 0.105$ Å^{-1}, was also found in the deuterated extract but only at 60°C (see Figs. 3 and 4).

Gerelli *et al.* · Neutron diffraction study of fully deuterated natural lipids

isotopic exchange (King & White, 1986). This analysis could only be applied to one of the detected d-spacings, namely d_a for the HRH sample at 18 and 30°C, as the patterns were characterized by three orders of diffraction. (3) expresses the SLD profile $\rho(z)$ along the normal to the substrate surface in relative units since the zeroth-order structure factor [$F(0)$ offset] and the absolute scaling of the Fourier series are unknown. These two quantities could be determined empirically knowing the minimum and maximum contrast values (Rappolt, 2010; Harroun *et al.*, 2008). The scaled curves are reported in Fig. 6.

Despite the low resolution of the resulting bilayer internal structure it was possible to obtain clear and useful information about the material repartition in the 105 Å d-spacing. The derived SLD profiles at the two temperatures (18 and 30°C) were almost identical, suggesting the absence of significant changes in the total structure of the bilayer. Phospholipid headgroups could be located at a distance of about ±27 Å from the centre of the repeating unit reported in Fig. 6, resulting in a bilayer thickness t_B of approximately 54 Å. The thickness of the water interlayer d_w turned out to be ∼51 Å ($d = t_B + d_w$). The value of t_B is in agreement with that obtained by neutron reflectometry measurements on the same natural lipid extracts (de Ghellinck, 2013). Moreover, this value lies in the typical range of thicknesses (50–80 Å) expected for natural membranes *in vivo* (Henderson, 1977; Korn, 1966; Fettiplace *et al.*, 1971; Meyer, 1979).

5. Discussion and conclusions

The availability of natural deuterated lipid extracts in large amounts will have a deep impact on biomembrane studies carried out using neutron scattering techniques. In the present
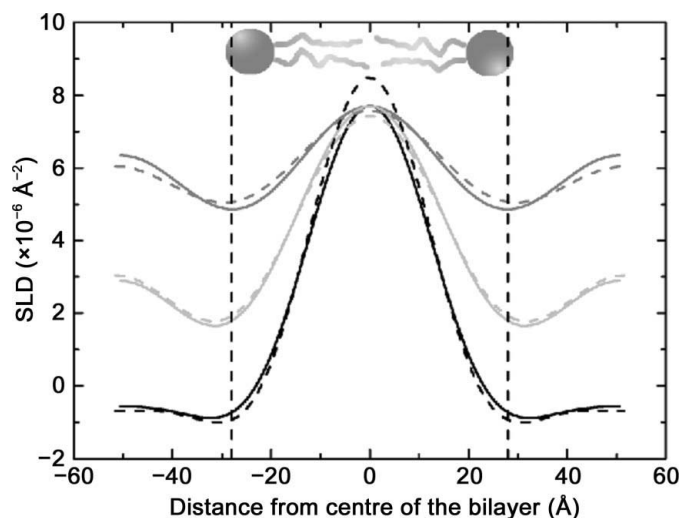

Figure 6
Scattering length density (SLD) profiles for a single deuterated bilayer as reconstructed according to (3). Different colours are used to indicate the hydration media (D$_2$O, grey; 1:1 H$_2$O:D$_2$O, light grey; H$_2$O, black), while different line types are used to indicate different temperatures (18°C, dashed lines; 30°C, continuous lines). Nonrealistic oscillations are induced into the profiles by Fourier series truncation to the third term (Rappolt, 2010). A schematic picture of two lipid molecules arranged as in a bilayer is shown to clarify the meaning of these SLD profiles.

work it is shown that full characterization of these extracts is necessary since the use of deuterated media during yeast cell growth affects the final lipid composition and, in turn, the structural features of the membrane. Lipid extracts from *P. pastoris* show different multi-lamellar arrangement for hydrogenous and deuterated samples. In both cases the heterogeneity in composition is reflected in significant structural complexity.

The diffraction patterns recorded for deuterated samples originated mainly from two different membrane stacks. At high relative humidity the sample was characterized by a lamellar arrangement showing two different periodicities. The shorter, designed d_b in the text, was present at 18 and 30°C but disappeared at 60°C, suggesting that the lipid moieties forming the d_b stack underwent a melting phase transition resulting in a molecular rearrangement in the sample. In fact, a simple gel-to-liquid transition (without molecular rearrangement) would lead to a shift of peak positions towards higher Q, *i.e.* relating to shorter distances in real space (Nallet *et al.*, 1993; White *et al.*, 1988). On the contrary, a stack associated with the d_b distance was also detected at the lower hydration levels at every temperature. The persistence of this diffraction feature could be interpreted as a humidity-induced modification of the melting point of the lipid involved in this kind of molecular arrangement. This is not surprising since it is known that the lipid-chain melting temperature increases upon dehydration (Koynova & Caffrey, 2002). The larger distance found in the high RH sample, d_a, was detected at all of the temperatures investigated, without any appreciable shift in the peak position. Nevertheless, a strong decrease in the diffracted intensity was observed at the higher temperature for all of the contrasts investigated. This may indicate disordering induced by larger thermal fluctuations. As described previously, the hydrogenous extracts were also characterized by the co-existence of lamellar stacks with different periodicities. At high relative humidity the features described for the deuterated extracts were also found in the data recorded for the hydrogenous extracts within a 5% difference in peak positions. Two additional stacking distances were present in the hydrogenous samples, suggesting a larger heterogeneity of the lamellar arrangement. In particular, the most intense peak for the hydrogenous extracts was related to a real-space distance of about 60 Å and therefore is in agreement with the typical d-spacing values characterizing stacks of zwitterionic phospholipids (Cavalcanti *et al.*, 2007; Trapp *et al.*, 2010; Schneck *et al.*, 2011; Steiner *et al.*, 2012; Foglia *et al.*, 2012; Knoll *et al.*, 2014). This feature was also present for a few deuterated samples and, in this case, the intensity of the peak was very close to the background level. At lower hydration the diffraction patterns of the two extracts were completely different. Those recorded for hydrogenous lipids were characterized by a single set of well defined peaks related to a single periodicity. This different behaviour is likely to be related to the differences in the fatty-acid distribution, leading to a difference in the phase diagrams of the two lipid extracts.

The lamellar arrangement of deuterated and hydrogenous lipid extracts from *P. pastoris* hydrated with pure water

mixtures indicate that the compositional heterogeneities were reflected in a structural heterogeneity that results in complex diffraction patterns. The values found for the main d-spacings were in agreement with what has previously been published for stacks of mixed polar and apolar phospholipid molecules.

The presence of multiple lamellar arrangements in the deuterated extracts could indicate the presence of lipid domains, characterized by different anionic/zwitterionic lipid ratios, in the plane of the bilayer. Nevertheless, no direct experimental observation of out-of-plane coherent scattering was detected to support this interpretation. Since all of the molecules in the samples were deuterated and since no large differences in chain length between anionic and zwitterionic lipids were expected, the presence of domains would not have been detectable using neutrons.

Only one deuterated sample, measured at high humidity, showed evidence of third-order diffraction. The Fourier synthesis of the repeating unit was carried out, even if only at low resolution. From the structure of this unit (see Fig. 6) the thickness of the bilayer was estimated to be approximately 54 Å; this is slightly larger than the values found for a pure DOPC bilayer (Wiener & White, 1992) but is very close to the thickness of a pure POPC bilayer (Gawrisch et al., 2007). In addition, the interface between the hydrophilic and hydrophobic parts of the bilayer was diffuse. This was induced by the presence of lipid species with slightly different chain lengths.

These systems provide an important comparison with the natural extracts investigated in the present work because oleic acid (C18:1) is the most abundant fatty-acid component in natural membranes (see Fig. 2b). Several different combinations of tails and headgroups are possible and these could explain the differences between the real and model systems. While the bilayer thickness is mainly dependent on the nature of the alkyl chain, the interaction between two successive membranes in the stack and therefore the thickness of the water layer between them depends mainly on the nature of the headgroup. Zwitterionic lipids in excess water conditions interact by van der Waals attraction and several repulsive forces. Equilibrium between these forces leads to well defined bilayer-to-bilayer distances. The corresponding water-layer thickness between adjacent zwitterionic lipid bilayers is typically between 10 and 30 Å depending on the exact lipid composition and phase (Aeffner, 2012). The presence of water molecules between two bilayers causes the so-called hydration repulsion effect (Israelachvili & Wennerstroem, 1992). The removal of water from these regions would reduce the overall repulsive force, promoting a thinning of the interbilayer distance d_w and therefore of the overall d-spacing. In the presence of charges, which are typically located in the headgroup region of lipid molecules, the repulsion is enhanced (Cowley et al., 1978). It has been shown that water repulsion becomes a minor force when charges are present on the membrane surface. The adsorption of two charges for every 60 lipid molecules on the membrane surface is able to produce an increase in the d-spacing of about 24 Å owing only to the increase of the thickness of the water layer (Schneck et al.,

2011). For the natural extracts studied here, the fraction of lipids with charged headgroups accounts for ∼25% of the total headgroup composition (see Fig. 2a). This could explain the larger d-spacing values observed in the current analysis. The reconstruction of the bilayer profile indicates that the water layer is ∼45 Å thick, a value larger than that commonly expected for stacks of zwitterionic membranes (Aeffner, 2012) but perfectly explicable by assuming strong electrostatic repulsion. This picture is also compatible with the small decrease in the d_a spacing upon dehydration. A similar system, composed of natural hydrogenous extracts, has been described by Cowley et al. (1978). PC and PG lipid moieties were extracted from eggs. They were both characterized by the distribution of chain pairs (data not reported). The features of the lamellar stack, especially the bilayer-to-bilayer separation distance, were analyzed as a function of the ratio between anionic and zwitterionic lipids, counter-ion concentration and hydration. When PG molecules were added at a level of more than 5% (by mole), a large swelling of the basic lamellar unit was observed for a given hydration level, indicating that electrostatic repulsion was the main repulsive force acting in the system. For some selected cases the d-spacing values reached 120 Å (Cowley et al., 1978). More recently it has been demonstrated that, for separation distances larger than 30 Å, the coexistence of electrostatic repulsion and of van der Waals attraction can promote a large but limited swelling in charged lipid mixtures characterized by PC and PS oleic-rich molecules (Steiner et al., 2012). On this basis, the presence of large d-spacings observed in all of the P. pastoris extracts can be understood. The addition of salt would screen the electrostatic repulsion, leading to smaller (and more common) d-spacing values.

This is the first published diffraction experiment on fully deuterated natural lipids; it has revealed that the membrane stack is complex and is regulated mainly by electrostatic repulsion between adjacent membranes, giving rise to large d-spacings. With a single exception, the number of orders of diffraction visible in the scattering patterns did not allow a detailed characterization of the internal structure of the lipid bilayer. Nevertheless, an approximate picture which provided useful information about the investigated systems was obtained. It must be mentioned that because of the structural heterogeneities in natural samples, the observation of up to the third order of diffraction is a significant. Further purification of the sample and isolation of selected lipid and phospholipid species will be necessary to obtain a greater level of detail on the sample stacking and on the internal structure of the bilayer. The combined use of neutron and X-ray diffraction will be necessary to achieve the highest possible resolution. In addition, similar experiments in the presence of physiological solutions (buffer, ionic strength etc.) will be performed to characterize these extracts under more biologically relevant conditions.

research papers

References

Aeffner, S. (2012). *Stalk Structures in Lipid Bilayer Fusion Studied by X-ray Diffraction*. Göttingen: Universitätsverlag Göttingen.

Blaurock, A. & Stoeckenius, W. (1971). *Nature New. Biol.* **233**, 152–155.

Büldt, G. & Seelig, J. (1980). *Biochemistry*, **19**, 6170–6175.

Caillé, A. (1972). *C. R. Acad. Sci.* **274**, 891–893.

Cavalcanti, L. P., Haas, H., Bordallo, H. N., Konovalov, O., Gutberlet, T. & Fragneto, G. (2007). *Eur. Phys. J. Spec. Top.* **141**, 217–221.

Cowley, A. C., Fuller, N. L., Rand, R. P. & Parsegian, V. A. (1978). *Biochemistry*, **17**, 3163–3168.

Demé, B., Cataye, C., Block, M. A., Maréchal, E. & Jouhet, J. (2014). *FASEB J.* **28**, 3373–3383.

Dencher, N. A., Dresselhaus, D., Zaccai, G. & Büldt, G. (1989). *Proc. Natl Acad. Sci. USA*, **86**, 7876–7879.

Devaux, P. F. (1991). *Biochemistry*, **30**, 1163–1173.

Devaux, P. F. (1992). *Annu. Rev. Biophys. Biomol. Struct.* **21**, 417–439.

Faber, K. N., Harder, W., Ab, G. & Veenhuis, M. (1995). *Yeast*, **11**, 1331–1344.

Fettiplace, R., Andrews, D. M. & Haydon, D. A. (1971). *J. Membr. Biol.* **5**, 277–296.

Foglia, F., Lawrence, M. J., Demé, B., Fragneto, G. & Barlow, D. (2012). *Sci. Rep.* **2**, 778.

Folch, J., Lees, M. & Sloane Stanley, G. H. (1957). *J. Biol. Chem.* **226**, 497–509.

Gawrisch, K., Gaede, H. C., Mihailescu, M. & White, S. H. (2007). *Eur. Biophys. J.* **36**, 281–291.

Ghellinck, A. de (2013). PhD thesis. Université Libre de Bruxelles, Belgium.

Ghellinck, A. de, Schaller, H., Laux, V., Haertlein, M., Sferrazza, M., Maréchal, E., Wacklin, H., Jouhet, J. & Fragneto, G. (2014). *PLoS One*, **9**, e92999.

Gordeliy, V. I. & Chernov, N. I. (1997). *Acta Cryst.* D**53**, 377–384.

Grage, S. L. et al. (2011). *Biophys. J.* **100**, 1252–1260.

Guinier, A. (1963). *X-ray Diffraction*. San Francisco: W. H. Freeman & Co.

Harroun, T. A., Katsaras, J. & Wassall, S. R. (2008). *Biochemistry*, **47**, 7090–7096.

Henderson, R. (1975). *J. Mol. Biol.* **93**, 123–138.

Henderson, R. (1977). *Annu. Rev. Biophys. Bioeng.* **6**, 87–109.

Huster, D., Jin, A. J., Arnold, K. & Gawrisch, K. (1997). *Biophys. J.* **73**, 855–864.

Ichihara, K. & Fukubayashi, Y. (2010). *J. Lipid Res.* **51**, 635–640.

Ikeda, M., Kihara, A. & Igarashi, Y. (2006). *Biol. Pharm. Bull.* **29**, 1542–1546.

Israelachvili, J. & Wennerstroem, H. (1992). *J. Phys. Chem.* **96**, 520–531.

Jacrot, B. (1976). *Rep. Prog. Phys.* **39**, 911–953.

Jouhet, J., Maréchal, E., Bligny, R., Joyard, J. & Block, M. A. (2003). *FEBS Lett.* **544**, 63–68.

King, G. I. & White, S. H. (1986). *Biophys. J.* **49**, 1047–1054.

Kirschner, D. A. & Caspar, D. L. (1972). *Ann. N. Y. Acad. Sci.* **195**, 309–320.

Knoll, W., Peters, J., Kursula, P., Gerelli, Y., Ollivier, J., Demé, B., Telling, M., Kemner, E. & Natali, F. (2014). *Soft Matter*, **10**, 519–529.

Korn, E. D. (1966). *Science*, **153**, 1491–1498.

Koynova, R. & Caffrey, M. (2002). *Chem. Phys. Lipids*, **115**, 107–219.

LeNeveu, D. M., Rand, R. P. & Parsegian, V. A. (1976). *Nature (London)*, **259**, 601–603.

Manno, S., Takakuwa, Y. & Mohandas, N. (2002). *Proc. Natl Acad. Sci. USA*, **99**, 1943–1948.

Maric, S., Skar-Gislinge, N., Midtgaard, S., Thygesen, M. B., Schiller, J., Frielinghaus, H., Moulin, M., Haertlein, M., Forsyth, V. T., Pomorski, T. G. & Arleth, L. (2014). *Acta Cryst.* D**70**, 317–328.

Maric, S., Thygesen, M. B., Schiller, J., Marek, M., Moulin, M., Haertlein, M., Forsyth, V. T., Bogdanov, M., Dowhan, W., Arleth, L. & Pomorski, T. G. (2014). *Appl. Microbiol. Biotechnol.*, doi: 10.1007/s00253-014-6082-z.

McDaniel, R. V. (1988). *Biochim. Biophys. Acta*, **940**, 158–164.

Meer, G. van, Voelker, D. R. & Feigenson, G. W. (2008). *Nature Rev. Mol. Cell Biol.* **9**, 112–124.

Meyer, R. A. (1979). *Appl. Opt.* **18**, 585–588.

Nagle, J. F. & Tristram-Nagle, S. (2000). *Biochim. Biophys. Acta*, **1469**, 159–195.

Nallet, F., Laversanne, R. & Roux, D. (1993). *J. Phys. IV*, **3**, 487–502.

Perino-Gallice, L., Fragneto, G., Mennicke, U., Salditt, T. & Rieutord, F. (2002). *Eur. Phys. J. E*, **8**, 275–282.

Rappolt, M. (2010). *J. Appl. Phys.* **107**, 084701.

Safinya, C. R., Roux, D., Smith, G. S., Sinha, S. K., Dimon, P., Clark, N. A. & Bellocq, A. M. (1986). *Phys. Rev. Lett.* **57**, 2718–2721.

Schneck, E., Demé, B., Gege, C. & Tanaka, M. (2011). *Biophys. J.* **100**, 2151–2159.

Sebastiani, F., Harvey, R., Khanniche, S., Artero, J., Haertlein, M. & Fragneto, G. (2012). *Eur. Phys. J. Spec. Top.* **213**, 355.

Simons, K. & Ikonen, E. (1997). *Nature (London)*, **387**, 569–572.

Simons, K. & Vaz, W. L. (2004). *Annu. Rev. Biophys. Biomol. Struct.* **33**, 269–295.

Spector, A. A. & Yorek, M. A. (1985). *J. Lipid Res.* **26**, 1015–1035.

Steiner, A. et al. (2012). *Langmuir*, **28**, 2604–2613.

Stoker, B., Roux, S. & Brown, W. (1978). *Nature (London)*, **271**, 180–182.

Tanford, C. (1980). *The Hydrophobic Effect: Formation of Micelles and Biological Membranes*, 2nd ed. New York: Wiley.

Trapp, M., Gutberlet, T., Juranyi, F., Unruh, T., Demé, B., Tehei, M. & Peters, J. (2010). *J. Chem. Phys.* **133**, 164505.

Tristram-Nagle, S. A. (2007). *Methods Mol. Biol.* **400**, 63–75.

White, S. H., Mirejovsky, D. & King, G. I. (1988). *Biochemistry*, **27**, 3725–3732.

Wiener, M. C. & White, S. H. (1992). *Biophys. J.* **61**, 434–447.

Worthington, C. R. (1969). *Biophys. J.* **9**, 222–234.

Wriessnegger, T., Leitner, E., Belegratis, M. R., Ingolic, E. & Daum, G. (2009). *Biochim. Biophys. Acta*, **1791**, 166–172.

Zaccai, G., Blasie, J. K. & Schoenborn, B. P. (1975). *Proc. Natl Acad. Sci. USA*, **72**, 376–380.

Zaccai, G., Büldt, G., Seelig, A. & Seelig, J. (1979). *J. Mol. Biol.* **134**, 693–706.

Zhang, R., Suter, R. & Nagle, J. (1994). *Phys. Rev. E*, **50**, 5047.